Ultrabright and Ultrafast III–V Semiconductor Photocathodes

Siddharth Karkare, Laurent Boulet, Luca Cultrera, Bruce Dunham, Xianghong Liu, William Schaff, and Ivan Bazarov
CLASSE, Cornell University, Ithaca, New York 14853, USA
(Received 18 November 2013; published 3 March 2014)

Crucial photoemission properties of layered III–V semiconductor cathodes are predicted using Monte Carlo simulations. Using this modeling, a layered GaAs structure is designed to reduce simultaneously the transverse energy and response time of the emitted electrons. This structure, grown by molecular beam epitaxy and activated to negative electron affinity, is characterized. The measured values of quantum efficiency and transverse energy are found to agree well with the simulations. Such advanced layered structures will allow generation of short electron bunches from photoinjectors with superior beam brightness.

DOI: 10.1103/PhysRevLett.112.097601 PACS numbers: 79.60.Dp, 07.77.Ka, 79.60.Jv

Photoemission-based electron sources can provide extremely bright beams with subpicosecond time resolution [1]. These sources enable applications such as ultrafast electron diffraction (UED) [2], inverse compton scattering [3], electron cooling of hadron beams [4], polarized electron beams for colliders, and modern light sources based on free-electron lasers [5] or energy recovery linacs [6].

The photocathodes used in these sources must meet a number of often conflicting requirements: high efficiency; prompt emission (response time); low emittance; and longevity. High quantum efficiency (QE) cathodes are desirable for applications with high average current or bunch charges. In order to reduce the demands on the drive laser, cathodes with QE values of 1% or greater are desirable [7]. Prompt emission implies that the electrons are emitted quickly after the incident photon pulse arrives at the cathode. Electrons excited deep within a cathode can take many tens of picoseconds to reach the surface and escape into vacuum, producing an undesirable time structure, while subpicosecond to picosecond time scales are needed for most applications. The emitted electron beam is contained within a phase space volume, known as the emittance [1]. The intrinsic emittance of the beam from a photocathode is determined by the laser beam size and the mean transverse energy (MTE) of the emitted electrons through the relation:

$$\epsilon_{n,x} = \sigma_{l,x}\sqrt{\frac{MTE}{m_e c^2}}, \tag{1}$$

where $\epsilon_{n,x}$ is the normalized transverse emittance in the x plane, $\sigma_{l,x}$ is the rms laser spot size, m_e is the electron mass, and c is the speed of light. The lower limit to laser spot size is given by the charge per bunch (q) required for the specific application and by the electric field E_{cath} at the cathode as $\sigma_{l,x} \approx \sqrt{\frac{1}{4\pi\epsilon_0}\frac{q}{E_{\mathrm{cath}}}}$, assuming a short duration uniform round laser spot [1]. The Value of the MTE, however, depends on the cathode material and can range from 25 meV up to 1 eV [8]. Finally, cathode longevity, or lifetime, implies that the photocathode is robust enough to operate in the environment of the application without significant QE degradation.

Finding a photocathode that simultaneously meets all of these requirements is difficult. For example, GaAs photocathodes have the lowest known MTE of 25 meV for laser excitation near the band gap, but have poor QE ($\leq 1\%$) and a slow response time [9]. Using a green wavelength excitation on GaAs, the QE is high and the photoemission in prompt, but the MTE is five times worse. Presently, no photocathode meets all of the stated requirements and tradeoffs must be made for each application.

For UED applications, the transverse coherence length ($L_\perp$) of the electron beam is important [10]. It is related to the beam emittance according to

$$L_\perp = \lambda\!\!\!^{-}\frac{\sigma_{e,x}}{\epsilon_{n,x}}, \tag{2}$$

where $\lambda\!\!\!^{-} = \frac{\hbar}{m_e c}$ is the reduced Compton wavelength and $\sigma_{e,x}$ is the rms size of the electron beam at the sample. This coherence length has to be of the order of the unit cell size of the molecule one is trying to resolve (~10 nm for proteins). Reducing MTE of the photocathodes to the < 10 meV range would accomplish this task in the modern photoemission guns used for UED. If the MTE is made even smaller (1–2 meV scale), other effects like disorder-induced heating [11], which are not directly related to the photocathodes themselves, come into play. However, no photocathode at the moment can demonstrate this low MTE simultaneously with a fast (< 1 ps) response time.

Reduction in MTE has been predicted from *ab initio* calculations of the surface band structure of Ag photocathodes with a thin layer of MgO [12]. However, such a photocathode has not been realized in practice. Furthermore, even with plasmonic QE enhancement

 © 2014 American Physical Society

[13], metallic photocathodes cannot provide sufficient QE to meet the requirements of high current applications [7]. QE greater than 1% in visible light can be obtained from III–V semiconductor photocathodes like GaAs activated to negative electron affinity (NEA) using Cs and NF_3 (or O_2) or from alkali antimonides with positive electron affinity. MTE reduction in GaAs is possible at longer wavelengths, but at the expense of other parameters. Alkali antimonides tend to have high surface roughness which limits the minimum MTE obtained to greater than 100 meV [14,15].

In the past, layered semiconductor structures consisting of GaAsP/GaAs and InGaAs/AlGaAs have been developed for polarized electron sources [16]. Complex III–V semiconductor structures consisting of AlGaAs and GaAs layers with graded doping have been grown and activated to NEA with the goal of maximizing QE [17]. QE in excess of 50% with 2.4 eV photons has been obtained [17]. However, the MTE and response time of such QE-enhanced layered structures remains unknown. Furthermore, theoretical models so far have been unable to quantitatively predict photoemission properties like QE, MTE, and response time from such photoemitters.

Recently, a quantitative agreement between theory and experiment has been obtained for these photoemission properties from NEA GaAs cathodes using a photoemission simulation that employs a semiclassical photoemission model using Monte Carlo based electron transport without the use of any *ad hoc* parameters [18]. In this Letter, this simulation tool has been extended to allow photoemission from III–V semiconductor layers with graded doping. Guided by the simulations, a layered structure with a lower MTE and response time has been engineered. The measured photoemission properties from this engineered photoemitter are found to be in excellent agreement with the simulations.

For the first time, we have proposed and demonstrated a reduction in MTE along with a possible reduction in response time of photocathodes, by controlling the surface band bending and transport properties of a layered semiconductor structure. This opens a way to systematic, theory-driven design of complicated layered structures of III–V semiconductors that exploit the band gaps, intervalley deformation potentials, and electron transport properties of different semiconductor materials along with graded doping for optimization of various photoemission properties. The use of such structures optimized for photoemission are expected to produce ultrabright and ultrafast electron bunches improving the performance in existing applications and enabling new ones.

The photoemission simulation approach [18] is based on Spicer's 3-step photoemission model [19]. Figure 1(a) shows the three steps of photoemission for *p*-doped GaAs. The first step is the excitation of electrons from the valence to the conduction band (process *A* in Fig. 1). The second step is the transport of excited electrons to the

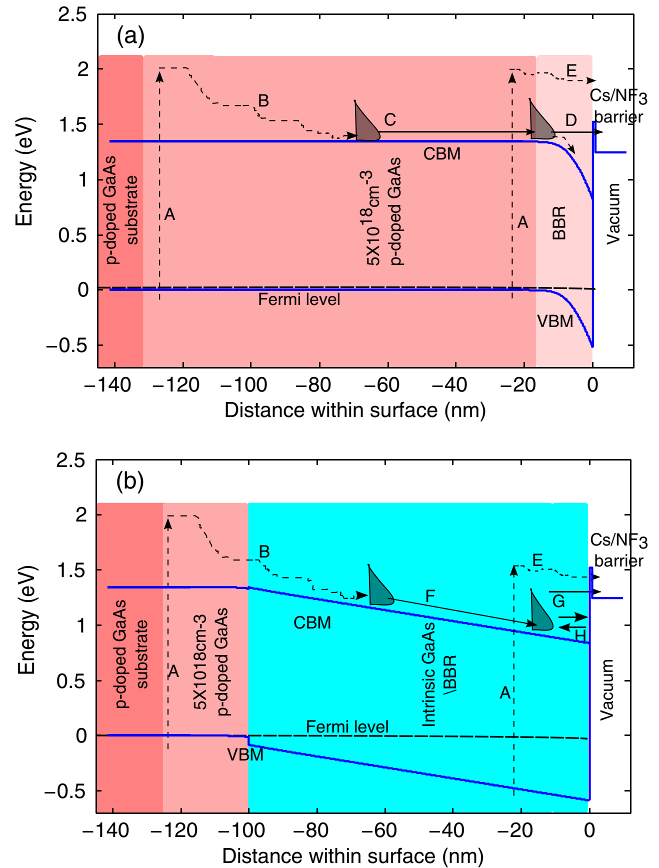

FIG. 1 (color online). Process of photoemission from (a) activated *p*-doped GaAs, (b) layered structure with 100 nm intrinsic GaAs. The various electron processes (indicated $A - H$) are described in the text.

surface (processes *B* and *C* in Fig. 1). During this step, the excited electrons scatter with phonons, holes, and other electrons, losing energy and thermalizing towards the conduction band minima (CBM). A 3D semiclassical electron transport model along with the 3-valley model for the conduction band structure is used to model this process. Scattering of electrons is taken into account using a Monte Carlo scheme. Scattering processes with acoustic, polar optical, and intervalley optical phonons as well as charged impurities and holes have been included. An electric field is applied to the electrons to simulate band bending near the surface. The third step is the emission of electrons into vacuum (process *D* in Fig. 1). Some electrons that are excited close to the surface reach vacuum without complete thermalization (process *E* in Fig. 1). Due to the activating layer of Cs and NF_3 (or O_2) on the surface, the vacuum level goes below the bulk conduction band minima (NEA condition). Electrons reaching the surface tunnel through a small barrier formed by the activating layer and are emitted into vacuum.

The small effective electron mass in the Γ valley of GaAs along with the conservation of transverse momentum at the surface should cause the MTE to be lower than 5 meV.

However, the measured values of MTE are an order of magnitude higher. This discrepancy is not well understood and has been attributed to surface roughness or surface scattering during emission [20]. In the simulations, this fact has been accounted for by introducing an elastic process that causes the electrons to be emitted in a cosine distribution about the normal to the surface (refer to [18] for details). The MTE values obtained from using this assumption are close to the experimental results. NEA, defined as the difference between the bulk CBM and the vacuum level, has a very strong dependence on the surface cleanliness, vacuum conditions, and the details of the activation procedure. This varies from sample to sample and from activation to activation and is difficult to reproduce exactly in experiment. The typical value of NEA may vary from 50 to 250 mV. In the simulation, the NEA is allowed to vary between these values to best fit the experimental data, but afterwards it is held fixed for any particular sample. Details of this simulation approach and its implementation have been presented elsewhere [18].

The simulation tool described above has been extended to handle layered structures. The energies of the Γ valley, L valley, X valley, and valence band maxima (VBM) as a function of the depth beneath the surface are calculated using a Schrödinger-Poisson solver [21]. We assume that the Fermi level at the surface is pinned to one third of the band gap above the valence band maxima at the surface due to the activation layer present [22]. The band gap renormalization due to high doping has been included [23]. The gradient of the valley minima gives the electric field applied to the electrons in that particular valley during the electron transport. Scattering is taken into account using the same Monte Carlo technique. The scattering rates have a spatial dependence in accordance with the layer material and doping level and the hole density obtained from the Schrödinger-Poisson solver.

The simulation model has several limitations. It does not include the effects of localized quantum states near the surface in the band bending regions. The transport of electrons is treated in a semiclassical fashion and does not include quantum tunneling and reflection except at the vacuum interface. The effects of quantum well states have also been ignored. The maximum photon energy that can be simulated is limited by the electron energies up to which the 3-valley model of the conduction band is valid. This limit is about 2.4 eV for GaAs. Despite these limitations, the simulations produce excellent agreement with the experimental data as discussed below.

Photoemission from a structure made of a layer of intrinsic GaAs over the bulk GaAs p-doped to 5×10^{18} cm^{-3} was simulated for an incident photon energy of 2.4 eV (photon energy of a standard frequency-doubled ytterbium fiber laser). Figure 1(b) shows the process of photoemission from this structure with a 100 nm thick intrinsic GaAs layer. The intrinsic GaAs layer causes the band bending region (BBR) to extend into the surface nearly to the entire depth of the intrinsic layer. This affects the excitation and transport properties and hence, changing the photoemission characteristics with the thickness of this layer. The dependence of QE, MTE, and response time on the thickness of this layer is shown in Fig. 2 for two values of NEA. Throughout this Letter, we quote the characteristic response time defined as the time required for about 57% of all photoemitted electrons to escape into vacuum assuming an infinitely short laser pulse [9].

In order to understand the effects of the intrinsic layer on emission, the emitted electrons can be roughly classified into two categories: (1) those that are excited close to the surface and get emitted before thermalizing; and (2) those that are excited deep within the surface and thermalize to the bulk CBM before emission. For a p-doped cathode without any intrinsic layer, the category 2 electrons dominate the emission. The BBR is small so these electrons do not get enough time to relax in it. As the thickness of the intrinsic layer increases more, category 2 electrons relax into the BBR (process F in Fig. 1). Most of these electrons do not have sufficient energy to escape and get trapped in the BBR (process H in Fig. 1), eventually recombining with holes. Some of the category 2 electrons do not relax sufficiently in the BBR and have a high enough energy to be emitted (process G in Fig. 1). This relaxation causes a number of the category 2 electrons to take a long time to reach the surface with insufficient energy to escape into vacuum. This explains the reduction of the QE and response time seen in Figs. 2(a) and 2(b).

The relaxation in the BBR also reduces the average energy of the emitted electrons. This causes the MTE to initially drop with increasing intrinsic layer thickness. However, as the thickness of this layer increases further, most of the category 2 electrons cannot be emitted, leading to the category 1 electrons to dominate the photoemission. These electrons are not thermalized and have a high energy when they reach the surface. This causes the MTE to eventually increase with the intrinsic layer thickness as seen in Fig. 2(c).

Thus, it is possible to reduce both MTE and response time simultaneously via an optimal choice of the intrinsic layer thickness. Even though this reduction is accompanied by a drop in QE, it still remains above the 1% level needed for many applications [7].

Guided by the simulations, a structure consisting of a 100 nm thick layer of intrinsic GaAs over the 5×10^{18} cm^{-3} p-doped bulk [Fig. 1(b)] was grown using molecular beam epitaxy (MBE). The sample was capped with a thick layer of As, removed from the MBE chamber, and transported in air into the GaAs activation chamber. The base vacuum in the GaAs activation chamber was 3×10^{-11} Torr. Here, the As cap was removed by heating the sample to 350°C for 2 hours, Thus preserving the

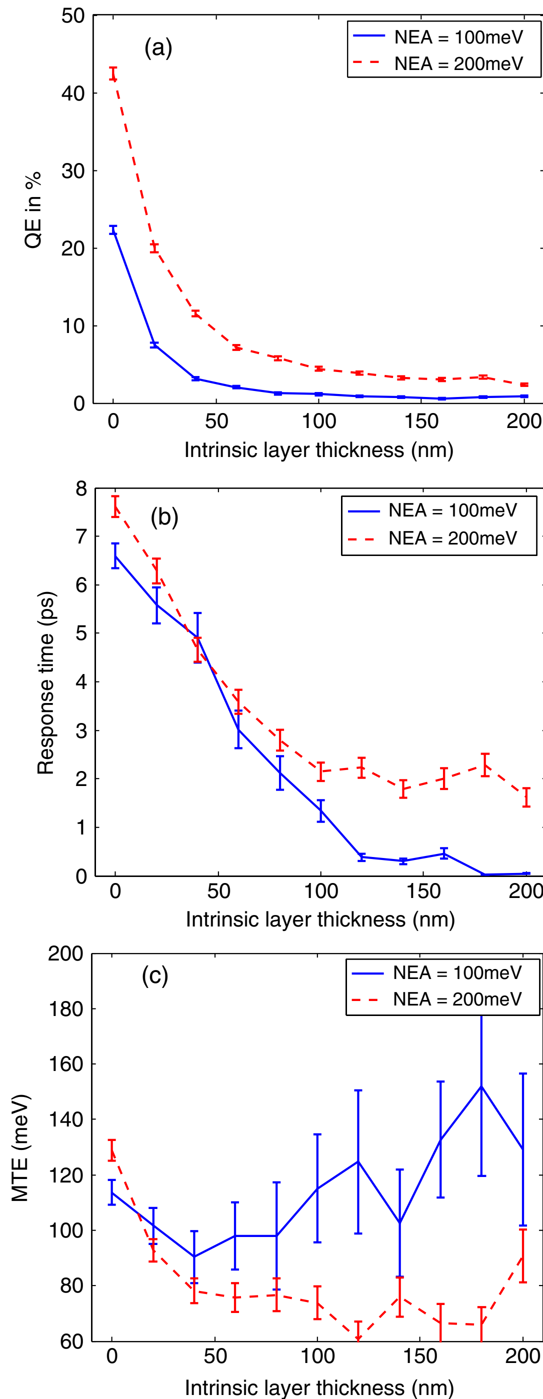

FIG. 2 (color online). Simulations of (a) QE, (b) response time, and (c) MTE as a function of the thickness of intrinsic GaAs layer for NEA of 100 and 200 meV. A thin layer of intrinsic GaAs on heavily p-doped GaAs causes the response time and MTE to reduce, changing them in a favorable way. The reduction in QE is unfavorable but can be tolerated for use in a photoinjector.

surface structure and cleanliness. The sample was activated to NEA using alternating exposures of Cs and NF_3 [24].

The spectral response was measured by collecting the current emitted from the activated sample while scanning the wavelength of the incident light. The activation chamber is connected in vacuum to a high voltage dc photogun [7]. Here, the MTE of emitted electrons was measured at various photon energies using a thoroughly benchmarked solenoid scan technique [9,14].

As a control, a GaAs wafer p-doped uniformly to 5×10^{18} cm^{-3} [Fig. 1(a)] was transported from the MBE chamber, cleaned, activated, and measured using the exact same procedure as the layered sample.

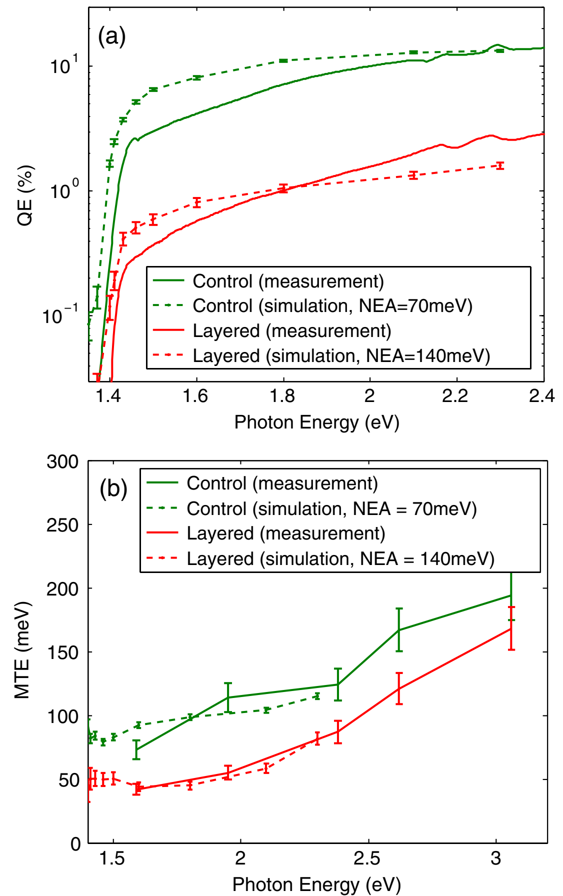

FIG. 3 (color online). (a) QE and (b) MTE as a function of incident photon energy for the two samples. The simulated results agree well with the experiment. The layered cathode shows a reduced QE with respect to the control sample. However, the QE is still greater than 1% in the green, exceeding the QE requirement of most photoinjectors [7]. NEA is fixed for a particular sample. It should be noted that the photon energy range above 2.4 eV is outside the validity of the 3-valley model for GaAs and cannot be simulated.

Figure 3 shows the spectral response and MTE measurements of this sample and the control sample along with the simulation results. NEA of 70 and 140 mV were used in the simulation to fit the data from the control and the layered samples, respectively. It is seen that the measured results are in excellent agreement with the simulations. The measurements show a 30%–50% drop in the MTE for the layered sample as compared to the control sample in the

red-green wavelengths. For a given bunch charge and a bunch frequency (determined by the application of the photoinjector), this results in a proportional increase in beam brightness [1,25].

In summary, using the Monte Carlo based photoemission simulation model, we designed a layered GaAs photocathode with reduced MTE and response time compared to the bulk GaAs. The structure was grown using MBE and activated to NEA. The measured QE and MTE agree well with the simulations. This and more advanced layered structures will be used to increase the electron beam brightness obtained from photoinjectors in the future.

This work has been funded by the NSF under Grant No. DMR-0807731 and DOE under Grant No. DE-SC0003965. The authors would like to thank Dr. Dimitre Dimitrov, Tech-X Corp, Boulder, Colorado, for many useful discussions.

[1] I. V. Bazarov, B. M. Dunham, and C. K. Sinclair, Phys. Rev. Lett. **102**, 104801 (2009).
[2] P. Musumeci, J. T. Moody, C. M. Scoby, M. S. Gutierrez, H. A. Bender, and N. S. Wilcox, Rev. Sci. Instrum. **81**, 013306 (2010).
[3] S. Boucher, P. Frigola, A. Murokh, M. Ruelas, I. Jovanovic, J. B. Rosenzweig, and G. Travish, Nucl. Instrum. Methods Phys. Res., Sect. A **608**, S54 (2009).
[4] I. Ben-Zvi *et al.*, Nucl. Instrum. Methods Phys. Res., Sect. A **532**, 177 (2004).
[5] W. Ackermann *et al.*, Nat. Photonics **1**, 336 (2007).
[6] S. M. Gruner, D. Bilderback, I. Bazarov, K. Finkelstein, G. Krafft, L. Merminga, H. Padamsee, Q. Shen, C. Sinclair, and M. Tigner, Rev. Sci. Instrum. **73**, 1402 (2002).
[7] B. Dunham *et al.*, Appl. Phys. Lett. **102**, 034105 (2013).
[8] D. H. Dowell, I. Bazarov, B. Dunham, K. Harkay, C. Hernandez-Garcia, R. Legge, H. Padmore, T. Rao, J. Smedley, and W. Wan, Nucl. Instrum. Methods Phys. Res., Sect. A **622**, 685 (2010).
[9] I. V. Bazarov, B. M. Dunham, Y. Li, X. Liu, D. G. Ouzounov, C. K. Sinclair, F. Hannon, and T. Miyajima, J. Appl. Phys. **103**, 054901 (2008).
[10] T. Van Oudheusden, E. F. de Jong, S. B. van der Geer, W. P. E. M. Op 't Root, O. J. Luiten, and B. J. Siwick, J. Appl. Phys. **102**, 093501 (2007).
[11] J. M. Maxson, I. V. Bazarov, W. Wan, H. A. Padmore, and C. E. Coleman-Smith, New J. Phys. **15**, 103024 (2013).
[12] K. Nemeth, K. C. Harkay, M. van Veenendaal, L. Spentzouris, M. White, K. Attenkofer, and G. Srajer, Phys. Rev. Lett. **104**, 046801 (2010).
[13] A. Polyakov, C. Senft, K. F. Thompson, J. Feng, S. Cabrini, P. J. Schuck, H. A. Padmore, S. J. Peppernick, and W. P. Hess, Phys. Rev. Lett. **110**, 076802 (2013).
[14] I. Bazarov, L. Cultrera, A. Bartnik, B. Dunham, S. Karkare, Y. Li, X. Liu, J. Maxson, and W. Roussel, Appl. Phys. Lett. **98**, 224101 (2011).
[15] L. Cultrera, I. Bazarov, A. Bartnik, B. Dunham, S. Karkare, R. Merluzzi, and M. Nichols, Appl. Phys. Lett. **99**, 152110 (2011).
[16] T. Nishitani *et al.*, J. Appl. Phys. **97**, 094907 (2005).
[17] Y. Zhang, B. Chang, J. Niu, J. Zhao, J. Zou, F. Shi, and H. Cheng, Appl. Phys. Lett. **99**, 101104 (2011).
[18] S. Karkare, D. Dimitrov, W. Schaff, L. Cultrera, A. Bartnik, X. Liu, E. Sawyer, T. Esposito, and I. Bazarov, J. Appl. Phys. **113**, 104904 (2013).
[19] W. E. Spicer, Appl. Phys. **12**, 115 (1977).
[20] S. Karkare and I. Bazarov, Appl. Phys. Lett. **98**, 094104 (2011).
[21] M. C. Foisy, Ph.D. thesis, Cornell University, 1990.
[22] J. J. Scheer and J. V. Laar, Solid State Commun. **5**, 303 (1967).
[23] H. S. Bennett, J. Appl. Phys. **83**, 3102 (1998).
[24] J. S. Escher, Semicond. Semimet. **15**, 195 (1981).
[25] C. Gulliford *et al.*, Phys. Rev. ST Accel. Beams **16**, 073401 (2013).